Supplementary Material (ESI) for Journal of Materials Chemistry

Supporting Information

Tuning Nanopatterns on Fused Silica Substrates: A Theoretical and Experimental Approach

Rodica Morarescu[1]*, Lars Englert[2], Branko Kolaric[1], Pascal Damman[1], Renaud A. L. Vallée[3], Thomas Baumert[2], Frank Hubenthal[2], and Frank Träger[2]

[1]Laboratoire Interfaces & Fluides Complexes, Centre d' Innovation et de Recherche en Matériaux Polymères, Université de Mons, 20 Place du Parc, B-7000 Mons, Belgium
[2]Institut für Physik and Center for Interdisciplinary Nanostructure Science and Technology (CINSaT), Universität Kassel, Heinrich-Plett-Str. 40, 34132 Kassel, Germany
[3]Centre de Recherche Paul Pascal (CNRS-UPR8641), 115 avenue du docteur Schweitzer, 33600 Pessac, France

1. Materials and Methods

1.1 Sample preparation

Regular arrays of triangular nanoparticles (NPs) were prepared by means of nanosphere lithography, a technique described in the literature [1, 2]. In brief, fused silica plates with an edge length of 12 mm served as substrates. The plates were cleaned in alkaline solutions (NaOH, KOH) for 20 minutes and subsequently 5 minutes in acid solution (HCL) to neutralize the substrate surface. Afterwards, the samples were placed in double-distilled water in an ultrasonic bath for 20 minutes. As a lithographic mask, monodisperse latex nanospheres (Microparticles) with a diameter of 330 nm were used. Large monolayer areas of well-ordered latex nanospheres have been prepared, utilizing the drop coating method of Micheletto et al. [2]. After formation of the nanosphere mask, the substrates were transferred in a thermal evaporation chamber (Balzers BA 510). At a pressure of 10^{-6} Pa gold atoms were deposited on the substrates with a rate of $\approx$ 0.2 nm/s. In all cases, the film thickness was set to 30 nm. Finally, the nanosphere mask was removed by sonicating the substrates for 3 minutes in dichloromethane, leaving behind large areas with highly ordered triangular gold NPs.

To create the nanopattern on the substrate surface, the samples were irradiated under ambient conditions with single light pulses with pulse duration of 35 fs (full width at

half maximum). After irradiation, the substrates were cleaned for 2 hours in aqua regia and subsequently sonicated for a few minutes in distilled water to remove residues of eventually remaining gold and ablated fused silica.

1.2 Laser system

Femtosecond laser light with a central wavelength of $\lambda \approx 790$ nm was provided by an amplified Ti:Sapphire laser system (Femtolasers Femtopower Pro), coupled to a modified microscope set up. Figure 1 depicts the experimental set up schematically. The laser light was expanded by a telescope system (not shown in Figure 1), to achieve a homogeneous illumination of the back aperture of the objective. Dispersive effects of the microscope system were compensated by a prism compressor of the laser amplifier. The laser light was focused by a Zeiss Epiplan 50x/0.5 NA objective (OB) on the sample surface (S). The substrate surface can be translated relative to the focal plane of the objective, leading to an increased spot diameter of 22 µm. The pulse duration was determined by autocorrelation measurements. The pulse energy has been adjusted by a motor driven gradient neutral density filter (GF) and recorded with a calibrated photodiode. Details of the laser set up have been described elsewhere [3].

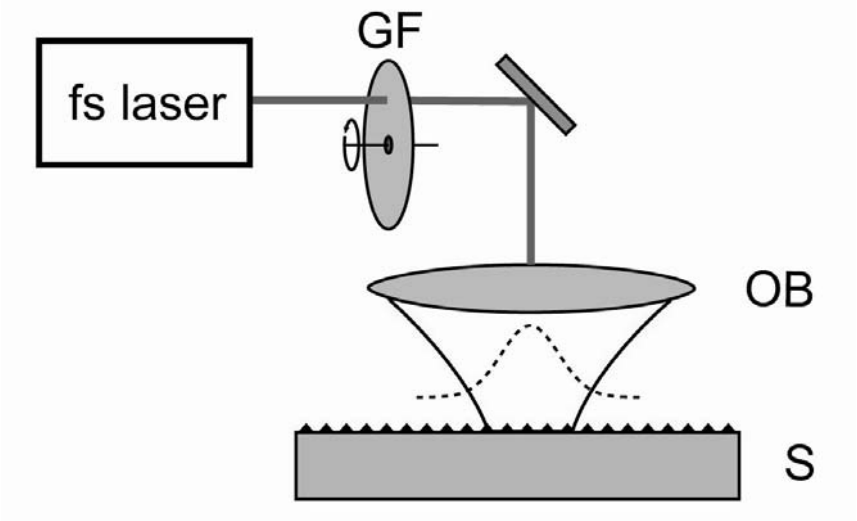

Fig. 1 Schematic of experimental set up. The energy of the fs-pulsed laser light is controlled by a neutral density gradient filter (GF) and focused by a microscope objective (OB) on the sample (S) containing the nanoparticles. The Gaussian intensity profile at the substrate surface is sketched (dashed line).

1.3 Laser treatment

To ensure the reproducibility of the experiments, in particular of the focusing conditions, the sample surface has been probed with a He-Ne laser in a confocal set up prior to

material processing. By placing the sample 20 μm ahead of the laser focus, the illuminated area on the sample surface was adjusted to 22 μm in diameter. Irradiation has been performed at normal incidence with linear or circular polarization. After applying a single pulse to one spot on a sample, the substrate has been translated by a 3-axis piezo table to a new position and another experiment has been performed. Along these lines, a complete set of experiments has been made with a single sample. In order to investigate how the generated nanopattern evolves as a function of laser energy, two strategies have been used. First, the intensity profile within the laser spot has been exploited. Due to the radial Gaussian intensity distribution, measurements at different distances from the center of the laser spot give nanostructures as a function of energy. Thus a full set of nanostructures on the substrates is obtained after a single shot experiment. In addition, to increase the energy range, the pulse energy has been varied from E = 0.1 μJ to E = 7.0 μJ.

1.4 Characterization

The samples have been investigated before and after irradiation with scanning electron (Hitachi S-4000) and atomic force microscopy (Thermo Microscopes, Autoprobe CP). Atomic force microscopy (AFM) has been applied to measure the dimensions of the NPs in the direction of the substrate normal as well as the dimensions of the created nanostructures on the substrate surface. The AFM measurements were performed under ambient conditions in non-contact mode using silicon tips (Veeco, Ultralevers, spring constant approximately 0.84 Nm^{-1}, resonance frequencies between 140 kHz and 180 kHz). Scanning electron microscopy (SEM) has been used to determine the lateral dimensions of the NPs and for large scale imaging of the generated nanostructures. After AFM characterization, the samples have been coated with a 2 nm thick gold layer to guarantee good conductivity for large scale SEM imaging. In addition, the triangular NP arrays were characterized by extinction spectroscopy, using a commercial spectrometer (Varian, Cary 100). Unpolarized light with an angle of incidence of 90° with respect to the sample surface was applied. Hence, only in-plane plasmon modes are detected.

1.5 Simulations

To relate the formation of these various nanopatterns as a result of the incoming polarization direction to the controlled directivity of the confinement and local enhancement of the electromagnetic field energy, we performed numerical simulations using the FDTD method. Such simulations [4] were made with a freely available software package [5]. Reflection spectra and mode profiles were obtained with a grid resolution of ≈ 3 nm. The dielectric permittivity of gold was determined using the Drude-Lorentz model with parameters determined by Vial et al. [6], based on the best fits, following a FDTD approach, to the relative permittivity of gold as tabulated by Johnson and Christy [7]. The wavelength λ = 705 nm used in the calculations corresponds to the dipolar plasmonic resonance of the triangle NPs as determined in preliminary reflection spectra calculations (not shown).

2. Experimental Results

2.1 Nanoparticle characterization

Figure 2a displays a large scale SEM image of the highly ordered triangular NPs. The inset in figure 2a shows a magnification, demonstrating that the NPs are triangular. Figure 2b depicts an AFM image of the same NPs. Due to the convolution of the NPs with the microscope tip, the NPs appear almost spherical. Therefore, only the dimension in the direction of the substrate normal of the triangular NPs has been obtained from the AFM images, while the lateral dimensions have been extracted from the SEM images. From the analysis of a set of such images an edge length of the NPs of (74 ± 6) nm and a height of (30 ± 4) nm has been determined. The tip to tip distance between two neighboring NPs amounts to (102 ± 14) nm. We emphasize that no damages of the gold NPs due to sonicating have been observed.

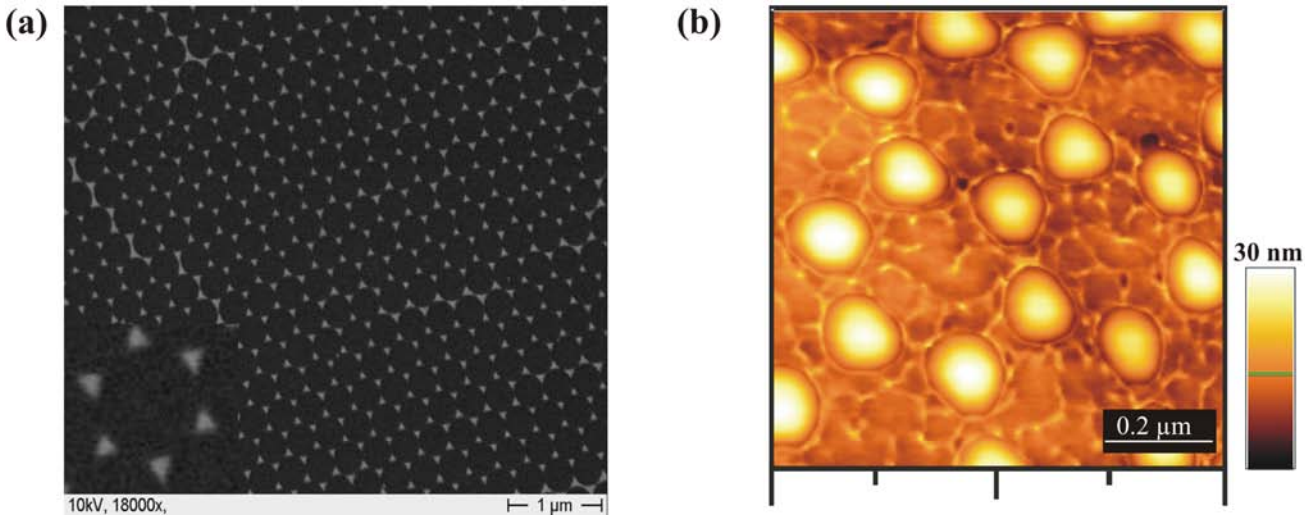

Fig. 2: (a) SEM image of the triangular NP array, demonstrating that the NPs are highly ordered on the substrate. (b) AFM image of the triangular NPs. The triangles appear almost spherical in shape due to convolution of the NPs with the AFM tip.

The extinction spectrum of a triangular NP array is depicted in figure 3. It shows a strong dipolar plasmon resonance at $\lambda = 730$ nm and a significantly less intense peak at $\lambda = 550$ nm, which can be attributed to excitation of a quadrupole mode [8, 9]. Hence, the wavelength of the applied laser light of $\lambda \approx 790$ nm excites the dipole mode of the triangular gold NPs.

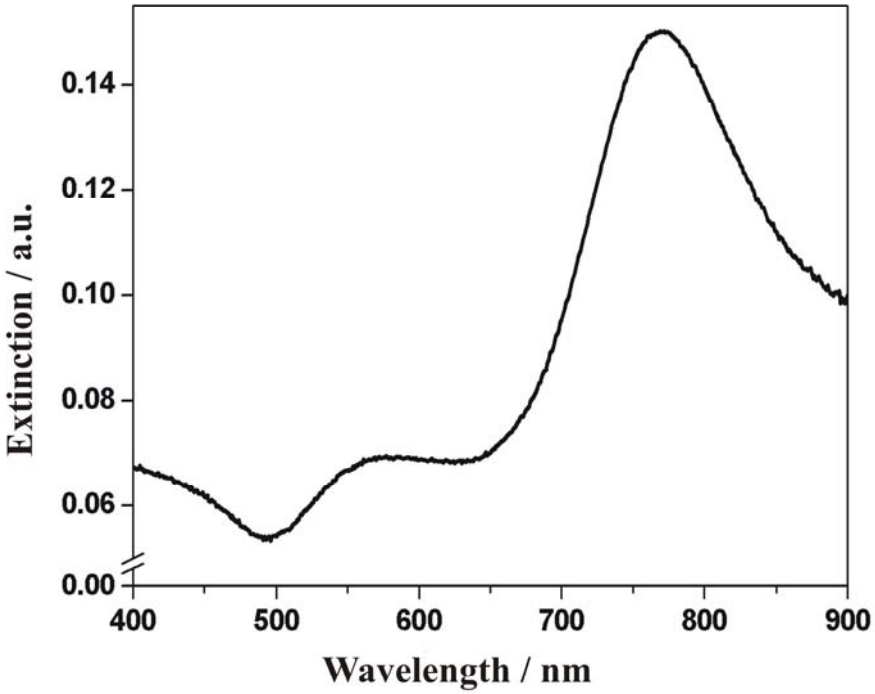

Fig. 3: Extinction spectrum of the triangular NP array. It exhibits a strong dipolar plasmon resonance at λ = 730 nm and a less pronounced resonance at λ = 550 nm, that is attributed to quadrupole excitation.

References

1. J. Hulteen, D. Treichel, M. Smith, M. Duval, T. Jensen, R. Van Duyne, J. Phys. Chem. B **103**, 3854 (1999).
2. R. Micheletto, H. Fukuda, M. Ohtsu, Langmuir **11**, 3333 (1995).
3. L. Englert, B. Rethfeld, L. Haag, M. Wollenhaupt, C. Sarpe-Tudoran, T. Baumert, Optics Express **15**, 17855 (2007).
4. A. Taflove, A. Hagness, S. C. Computational Electrodynamics: The Finite-Difference Time-Domain Method, 3rd ed.; Artech House, Inc.: Norwood, MA, (2005).
5. A. F. Oskooi, D. Roundy, M. Ibanescu, P. Bermel, J. D. Joannopoulos, S. G. Johnson, Comput. Phys. Commun. **181**, 687 (2010).
6. A. Vial, A.-S. Grimault, D. Macías, D. Barchiesi, M. Lamy de la Chapelle, Phys. Rev. B **71**, 085416 (2005).
7. P. Johnson and R. Christy, Phys. Rev. B **6**, 4370 (1972).
8. L. J. Sherry, R. Jin, C. A. Mirkin, G. C. Schatz, R. P. V. Duyne, Nano Lett. **6**, 2060 (2006).
9. K. L. Shuford, M. A. Ratner, G. C. Schatz, J. Chem. Phys. **123**, 114713 (2005).